

Tumor microenvironment characterization identifies two lung adenocarcinoma subtypes with specific immune and metabolic state

Jianbing Huang | Jiagen Li | Sufei Zheng | Zhiliang Lu | Yun Che |
 Shuangshuang Mao  | Yuanyuan Lei | Ruochuan Zang | Chengming Liu |
 Xinfeng Wang | Lingling Fang | Nan Sun | Jie He 

Department of Thoracic Surgery, National Cancer Center/National Clinical Research Center for Cancer/Cancer Hospital, Chinese Academy of Medical Sciences and Peking Union Medical College, Beijing, China

Correspondence

Nan Sun and Jie He, Department of Thoracic Surgery, National Cancer Center/National Clinical Research Center for Cancer/Cancer Hospital, Chinese Academy of Medical Sciences and Peking Union Medical College, Beijing 100021, China.
 Email: sunnan@vip.126.com (NS); prof.jiehe@gmail.com (JH)

Funding information

National Natural Science Foundation of China, Grant/Award Number: 81802299, 81502514; Fundamental Research Funds for the Central Universities, Grant/Award Number: 3332018070; CAMS Innovation Fund for Medical Sciences, Grant/Award Number: 2016-I2M-1-001, 2017-I2M-1-005; National Key Research and Development Program of China, Grant/Award Number: 2016YFC0901401; National Key Basic Research Development Plan, Grant/Award Number: 2018YFC1312105

Abstract

The tumor microenvironment (TME) is a vital component of tumor tissue. Increasing evidence suggests their significance in predicting outcomes and guiding therapies. However, no studies have reported a systematic analysis of the clinicopathologic significance of TME in lung adenocarcinoma (LUAD). Here, we inferred tumor stromal cells in 1184 LUAD patients using computational algorithms based on bulk tumor expression data, and evaluated the clinicopathologic significance of stromal cells. We found LUAD patients showed heterogeneous abundance in stromal cells. Infiltration of stromal cells was influenced by clinicopathologic features, such as age, gender, smoking, and TNM stage. By clustering stromal cells, we identified 2 clinically and molecularly distinct LUAD subtypes with immune active and immune repressed features. The immune active subtype is characterized by repressed metabolism and repressed proliferation of tumor cells, while the immune repressed subtype is characterized by active metabolism and active proliferation of tumor cells. Differentially expressed gene analysis of the two LUAD subtypes identified an immune activation signature. To diagnose TME subtypes practically, we constructed a TME score using principal component analysis based on the immune activation signature. The TME score predicted TME subtypes effectively in 3 independent datasets with areas under the receiver operating characteristic curves of 0.960, 0.812, and 0.819, respectively. In conclusion, we proposed 2 clinically and molecularly distinct LUAD subtypes based on tumor microenvironment that could be valuable in predicting clinical outcome and guiding immunotherapy.

KEYWORDS

lung adenocarcinoma, signature, subtype, tumor immunity, tumor microenvironment

Abbreviations: AUC, area under the ROC curve; DEG, differentially expressed gene; GEO, Gene Expression Omnibus; LUAD, lung adenocarcinoma; MSC, mesenchymal stem cell; NSCLC, non-small-cell lung cancer; PCA, principal component analysis; PD-1, programmed cell death-1; RNA-seq, RNA sequencing; ROC, receiver operating characteristic; TCA, tricarboxylic acid; TCGA, The Cancer Genome Atlas; Th, T helper; TME, tumor microenvironment.

This is an open access article under the terms of the Creative Commons Attribution-NonCommercial-NoDerivs License, which permits use and distribution in any medium, provided the original work is properly cited, the use is non-commercial and no modifications or adaptations are made.

© 2020 The Authors. *Cancer Science* published by John Wiley & Sons Australia, Ltd on behalf of Japanese Cancer Association.

1 | INTRODUCTION

Cancers develop in complex TMEs consisting of diverse immune cells, vasculature and ECM, which impact cancer cell survival, tumor metastasis, therapeutic efficiency, and patient outcome.¹ In TMEs, there exist a profound interaction network among cancer cells, stromal cells, and ECM. The TME has diverse capacities to exert both beneficial and adverse impact on tumorigenesis. Infiltrating immune cells could exert antitumor effects; in contrast, cancer cells could educate stromal cells, such as macrophages, neutrophils, and fibroblasts, to promote tumor growth and metastasis.²

Emerging evidence supports that TME plays a crucial role in therapeutic responses and patient outcome.^{3,4} The TME context reflects the tumor immune response⁵ and predicts therapeutic benefit.⁶ Immunotherapy has emerged as a new treatment arsenal in cancer, especially immune checkpoint inhibitors that unleash the antitumor immune response. Immune checkpoint inhibitors achieved success in cancer therapy, especially in melanoma and lung cancer where anti-PD-1 Abs have become part of the approved treatment. However, approximately 20% of the patients benefit from immune checkpoint inhibitors.⁷ Successful tumor elimination by immunotherapy requires the activation of the immune system. Unfortunately, exhausted or short-lived activation of immune cells and inhibitory microenvironment formation leads to resistance to immunotherapy.⁸ In addition to its effects on immunotherapy, TME influences the efficiency of chemotherapy and radiotherapy through preexisting TME properties and therapy-induced responses in TME.⁹ Infiltrating numbers of T cells, macrophages, and cancer-associated fibroblasts in the TME are associated with patient outcomes in various cancers, including lung cancer, urothelial cancer, and esophageal cancer.¹⁰⁻¹² Therefore, characterization of the TME facilitates the development of prognostic and predictive biomarkers and the identification of novel therapeutic targets.

Lung cancer is the leading cause of cancer-related death around the world.¹³ Lung adenocarcinomas constitute unique lung cancer subtypes with distinct cellular and mutational landscapes.¹⁴ Due to the anatomical structure of the lung, LUAD has a complex immune contexture. Emerging evidence supports that TME impacts LUAD progression and clinical outcome.¹ Here, we systematically profiled the stromal cell landscape of TME in 1184 lung adenocarcinomas using computational algorithms based on bulk tumor expression data,¹⁵ and correlated the stromal cell pattern with clinical and pathologic features. Based on the stromal cell profile, we identified and characterized 2 clinically and molecularly distinct LUAD subtypes with immune active and immune repressed features that could be valuable in predicting clinical outcome and guiding immunotherapy.

2 | MATERIALS AND METHODS

2.1 | Lung adenocarcinoma datasets and preprocessing

We systematically searched for LUAD gene expression datasets that were publicly available with full clinical information in GEO ([https://](https://www.ncbi.nlm.nih.gov/geo/)

www.ncbi.nlm.nih.gov/geo/) and TCGA. The results obtained many LUAD datasets with prognostic information. For controlling the data heterogeneity, finally, we included 3 treatment-naive LUAD cohorts with the most patients: GSE31210 (N = 226), GSE68465 (N = 443), and TCGA-LUAD (N = 515). The raw data for the dataset from Affymetrix were downloaded from GEO and processed using the RMA algorithm in the *affy* software package.¹⁶ Level 3 RNA-seq data (RSEM normalized) for genes and clinical information of TCGA-LUAD samples were downloaded from the UCSC Xena browser (<http://xena.ucsc.edu/>). Detailed information of included datasets is summarized in Table S1.

2.2 | Inference of infiltrating cells in TME

To quantify the abundance of tumor stromal cells in LUAD patients, we used the xCell algorithm, which allows for highly sensitive and specific inference of 64 stromal cell types from bulk tumor expression data.¹⁵ xCell is a gene signature-based method that integrates the advantages of gene set enrichment with deconvolution approaches, fitting RNA-seq and microarray data. Gene expression profiles were prepared according to the xCell instructions, and uploaded to the xCell web portal (<http://xcell.ucsf.edu/>), undertaken using the xCell signature (N = 64) with 1000 permutations. For the specific analysis of tumor stromal cells in LUAD, we finally included 43 cell types in our study (detailed information in Table S2).

2.3 | Consensus clustering for TME-infiltrating cells

Tumors with qualitatively different TME cell patterns were grouped using hierarchical agglomerative clustering. A consensus clustering algorithm was applied to determine the number of clusters in the TCGA-LUAD and meta-GEO dataset (GSE31210 and GSE68465), undertaken using the *ConsensusClusterPlus* R package with 1000 permutations.¹⁷

2.4 | Differentially expressed genes and signature genes analysis

Differentially expressed genes between different TME clusters were analyzed using R package *limma*, with an adjusted *P* less than .05.¹⁸ The adjusted *P* value for multiple testing was obtained using the Benjamini-Hochberg correction. Then we used the random forest classification algorithm to perform dimensionality reduction on DEGs in order to obtain signature genes between different TME clusters.¹⁹ After obtaining the signature genes, the *clusterProfiler* R package²⁰ was applied to annotate gene function with a *P* less than .01 and false discovery rate less than 0.05. Next, a consensus clustering algorithm was used to cluster the LUAD patients based on the signature genes. Then PCA was carried out for each LUAD patient based on the signature genes, and principal component 1 was extracted to serve as

the signature gene score for each patient.^{21,22} The obtained signature gene score was used to represent the signature of TME cluster and was defined as the TME score for each patient.

2.5 | Statistical analysis

For comparisons of 2 groups, unpaired Student's *t* tests and Mann-Whitney *U* tests were used to estimate normally distributed and nonnormally distributed variables, respectively. Correlation coefficients were computed by Spearman correlation analyses. The *p*ROC package²³ was used to plot ROC curves and calculate the AUCs to evaluate the diagnostic value of the TME score. The Kaplan-Meier method was applied to generate survival curves, with the log-rank (Mantel-Cox) test used to determine the statistical significance. *P* values were 2-sided and values less than .05 were considered statistically significant. All statistical analyses were undertaken using R (<https://www.r-project.org/>).

3 | RESULTS

3.1 | Landscape of TME cells in lung adenocarcinoma

To analyze the landscape of tumor stromal cells in lung adenocarcinoma, we collected a TCGA-LUAD dataset and a meta-GEO dataset (GSE31210 and GSE68465). The stromal cell pattern was portrayed using the xCell algorithm, which infers tumor stromal cells based on bulk tumor expression data (Table S3).¹⁵ The TME landscape of TCGA-LUAD (*N* = 515) is shown in Figure S1A and the meta-GEO dataset (*N* = 669) in Figure S1B. We found there was a heterogeneity of stromal cell patterns among LUAD patients, in that some patients were rich in stromal cells whereas others were not. We next correlated stromal cells with clinicopathologic characteristics in both TCGA and GEO datasets (Figure S1C). We found gender showed a negative correlation with many stromal cells, such as conventional dendritic cells, activated dendritic cells, naive B cells, and CD4⁺ naive T cells (Figure S1C), which means male patients have less infiltration of these cells in tumor tissue. The result indicated that infiltration of MSCs and Th1 cells decreased with aging, while mast cell increased with aging. Moreover, smoking increased the infiltration of plasma cells, Th2 cells, and pro-B cells, but decreased the infiltration of conventional dendritic cells. The correlation analysis between stromal cells and TNM stage showed that many immune cells decreased in advanced stage, such as B cells, CD4⁺ T cells, CD8⁺ T cells, and dendritic cells, while some immune cells increased in advanced stage, such as Th1 cells and Th2 cells.

3.2 | Identification of 2 TME subtypes of LUAD

Considering the heterogeneity of infiltrating stromal cells in LUAD (Figure S1), we wondered whether there are any TME subtypes of

LUAD patients. We assessed potential clusters using the consensus clustering method based on stromal cells,¹⁷ and obtained 2 stable clusters in both TCGA and meta-GEO datasets (Figure 1A, Table S3), termed TME cluster A and TME cluster B. We found that TME cluster A was rich in stromal cells and TME cluster B was poor in stromal cells (Figures 1B and S2A). Tumor microenvironment cluster A was distinguished by rich infiltrations of various immune cells, whereas TME cluster B was poor in most stromal cells, except that MSCs were higher in TME cluster B (Figure 1C). Furthermore, TME cluster A had significantly longer overall survival and disease-free survival than TME cluster B (Figures 1D and S2B).

3.3 | Immune and metabolic state of the 2 LUAD subtypes

To illustrate the underlying biological characteristics of the two TME phenotypes, we undertook DEG analysis on TCGA dataset, which contained more comprehensive patient information. We obtained 12 380 DEGs between 2 TME phenotypes, with 4409 genes upregulated in TME cluster A and 7971 genes upregulated in TME cluster B (Figure 2A, Table S4). The most significant DEGs were upregulated genes in TME cluster A, such as *CD4* (T-cell surface glycoprotein CD4), *CD200R1* (CD200 receptor 1), *CCL13* (C-C motif chemokine ligand 13), and *IGSF6* (Ig superfamily member 6), which are immune regulatory genes, and *FOLR2* (folate receptor beta), *MRC1* (mannose receptor C-type 1), *F13A1* (transglutaminase A chain), and *P2RY12* (purinergic receptor P2Y12), which are metabolism regulatory genes (Figure 2A).

To further investigate the immune status of the 2 distinct TME subtypes, we analyzed the expression profiles of 756 immune-related genes curated from the nCounter PanCancer Immune Profiling Panel (Table S4).²⁴ We found that the overall expression of immune-related genes was higher in TME cluster A than TME cluster B (Figure 2B). Moreover, we analyzed the expression patterns of immune checkpoint genes, including *PDCD1* (programmed cell death 1), *CD274* (programmed cell death 1 ligand 1), *PDCD1LG2* (programmed cell death 1 ligand 2), *CTLA4* (CTL associated protein 4), *CD80* (B7-1 antigen), *CD86* (B7-2 antigen), *HAVCR2* (hepatitis A virus cellular receptor 2, TIM-3), and *LGALS9* (galectin). The results showed that all analyzed immune checkpoints were significantly overexpressed in TME cluster A than TME cluster B except galectin-9 (Figure 2C). Infiltrating stromal cells are recruited by chemokines and cytokines. We therefore investigated whether there was a distinct chemokine/cytokine microenvironment in each TME subtype. We found that expression of C-C motif chemokines and C-X-C motif chemokines was higher in TME cluster A than TME cluster B (Figure 2D).

Previous study indicates that immune responses are largely shaped by cell metabolism²⁵; we therefore explored the metabolomic variations between the 2 TME subtypes by analyzing the expression of 2031 metabolism-related genes obtained from the ccmGDB database (Table S4).²⁶ The result revealed that there

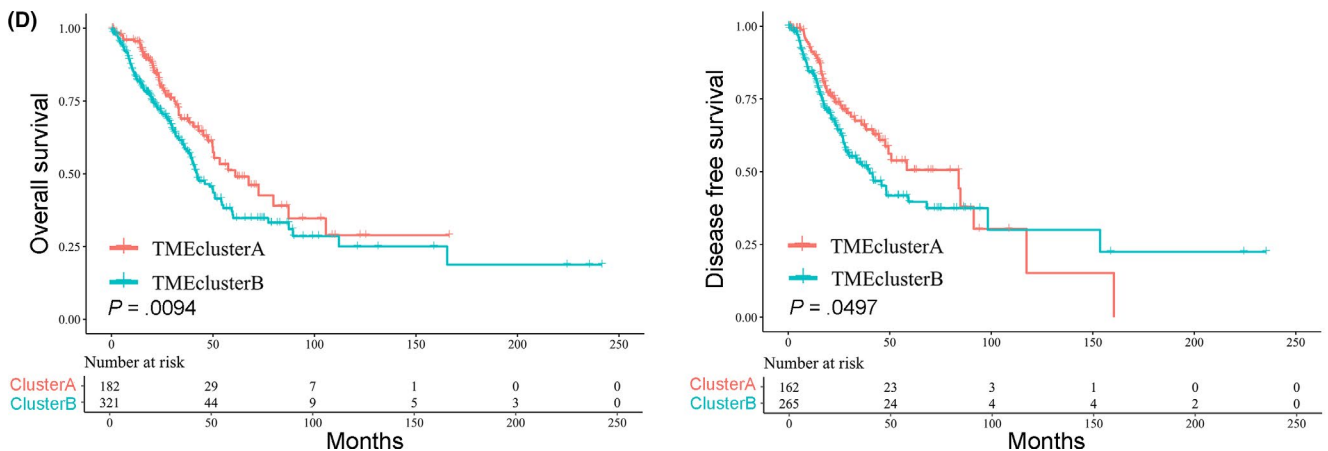
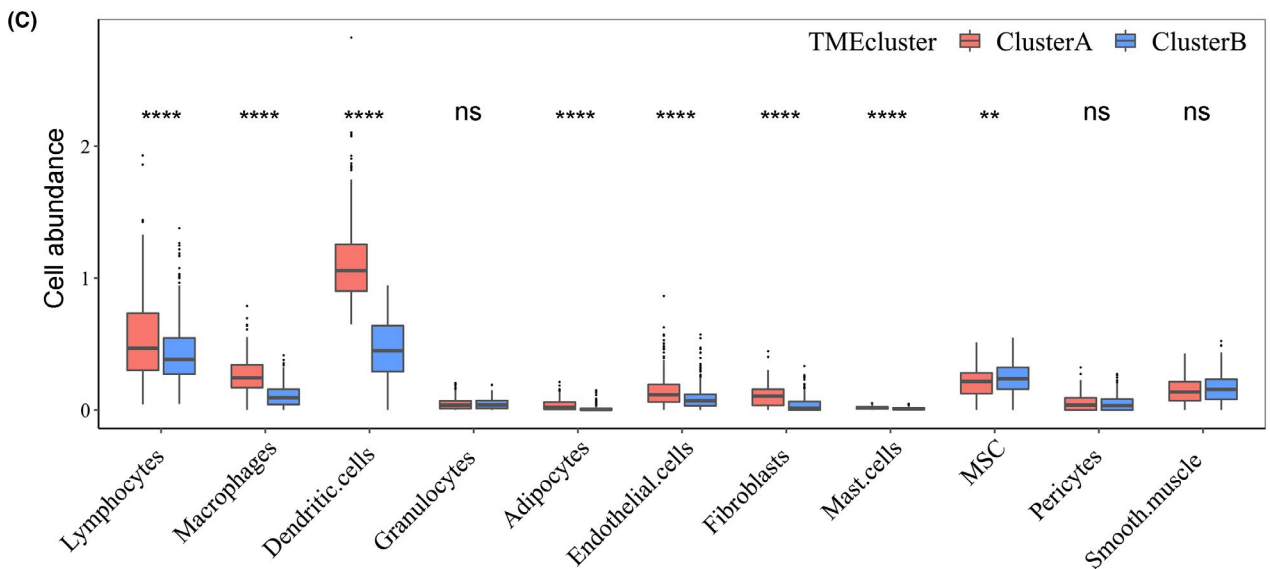
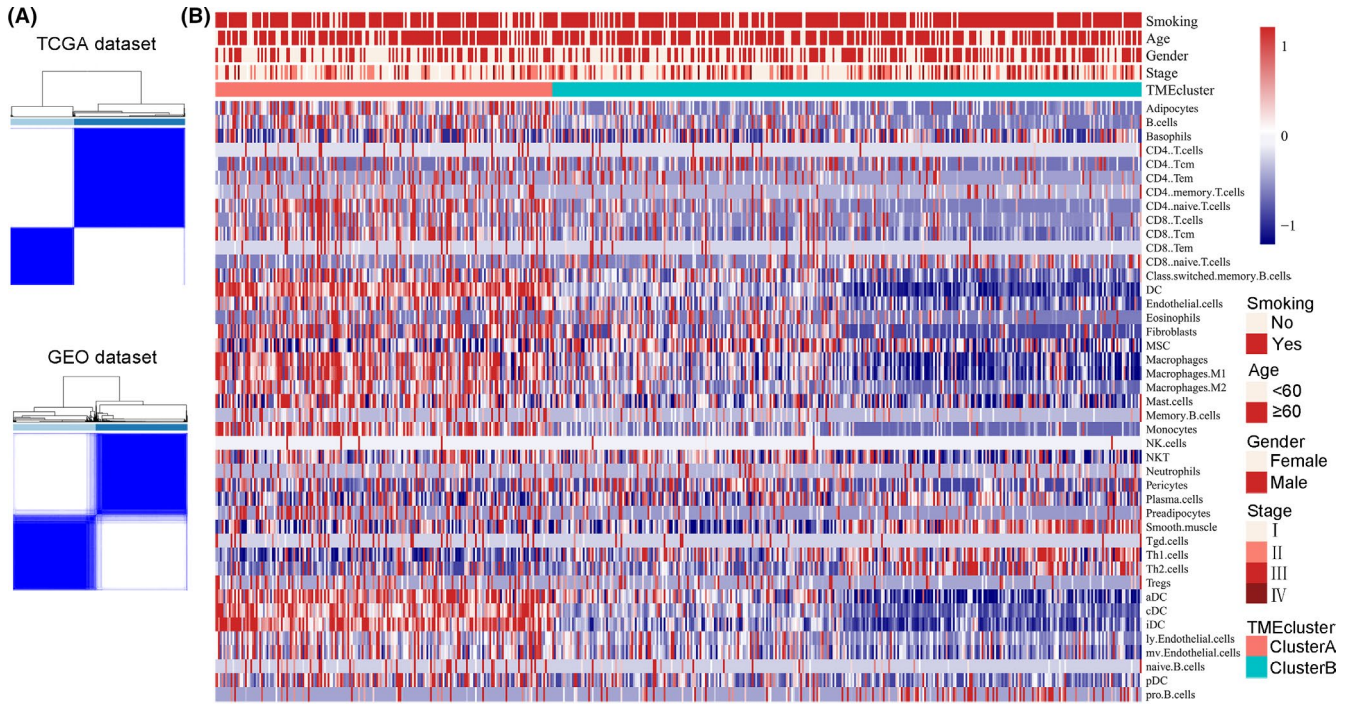


FIGURE 1 Identification of 2 tumor microenvironment (TME) subtypes in lung adenocarcinoma. A, Consensus matrixes of lung adenocarcinoma in The Cancer Genome Atlas (TCGA) and Gene Expression Omnibus (GEO) datasets revealed 2 TME subtypes, using 1000 iterations of hierarchical clustering. B, Unsupervised clustering of TME cells for 515 patients in TCGA cohort. Smoking, age, gender, stage, and TME cluster are shown as patient annotations. Top legend, white indicates missing value. C, TME cell abundance in different TME clusters. *P* values obtained using Student's *t* test (2-tailed). ***P* < .01, ****P* < .0001. ns, nonsignificant. D, Kaplan-Meier curves for overall survival (left panel) and disease-free survival (right panel) of lung adenocarcinoma patients in TCGA cohort. *P* values were obtained using the log-rank test

were more overexpressed metabolism-related genes in TME cluster B than TME cluster A (1018 upregulated genes in cluster B, 352 upregulated genes in cluster A) (Figure 3A). Next, we carried out GO and Kyoto Encyclopedia of Genes and Genomes enrichment analysis of upregulated metabolism-related genes in each TME cluster. Tumor microenvironment cluster A showed enrichment of glycosaminoglycan, aminoglycan, and glycerolipid metabolism process (Figure 3B). Tumor microenvironment cluster B showed enrichment of diverse metabolic pathways, including carbohydrate metabolism, amino acid metabolism, nucleic acid metabolism, and the citrate cycle (TCA cycle) (Figure 3C). Cellular proliferation is largely dependent on cell metabolic status.²⁵ Therefore, we investigated the expression of proliferation markers in 2 TME subtypes, including MKI67 (marker of proliferation Ki-67), PCNA (proliferating cell nuclear antigen), and MCM (minichromosome maintenance complex component) family genes.²⁷ We found that all proliferation markers were significantly overexpressed in TME cluster B except MCM5 (minichromosome maintenance complex component 5) (Figure 3D). Taken together, these results suggested that TME cluster A was characterized by active immune response and repressed metabolism, whereas TME cluster B was characterized by repressed immune response and active metabolism.

3.4 | Phenotype signature of the 2 LUAD subtypes

To figure out the gene expression difference between TME cluster A and TME cluster B, we undertook dimensionality reduction to extract the phenotype signatures using the random forest algorithm based on the 12 380 DEGs.²⁸ We obtained 193 signature genes, with 184 genes upregulated in TME cluster A and 9 genes upregulated in TME cluster B (Table S5). Then we focused on the upregulated signature genes in TME cluster A, and undertook GO enrichment analysis. The signature genes showed an enrichment of proliferation and activation of immune cells (Figure 4A). The unsupervised hierarchical cluster analysis based on the expression of the 184 signature genes separated the TCGA-LUAD cohort population into 2 distinct patient clusters, termed Gene cluster A and Gene cluster B. Consistent with the results of the TME phenotypes, Gene cluster A showed highly expressed signature genes and Gene cluster B showed repressed expression of signature genes (Figure 4B). Moreover, Gene cluster A showed more infiltration of diverse immune and stromal cells (Figure 4C). Overexpression of genes involved in immune activation, which were enriched in Gene cluster A, correlated with a good prognosis in LUAD (Figure 4D).

Therefore, we identified an immune activation signature distinguishing TME cluster A with TME cluster B.

3.5 | TME score predicted TME phenotypes in LUAD

To apply the novel TME classification practically, we constructed the TME score using the PCA algorithm based on the TME signature genes, which could represent the signature of TME clusters (Table S5). We found that the TME score was significantly higher in TME cluster A than TME cluster B in 3 independent datasets, including TCGA-LUAD, GSE31210, and GSE68465 (Figure 5A). Then we evaluated the diagnostic value of the TME score in TME clusters using ROC analysis. The TME score showed high diagnostic value in TME cluster diagnosis in 3 independent datasets (AUC = 0.960 in TCGA-LUAD, AUC = 0.812 in GSE31210, and AUC = 0.819 in GSE68465) (Figure 5B-D). Collectively, the TME score predicted TME phenotypes in LUAD.

4 | DISCUSSION

Lung cancer is one of the deadliest cancers around the world and LUAD constitutes the major pathologic subtype with distinct cellular and mutational landscape. Lung adenocarcinoma is a heterogeneous disease on the molecular level; according to our study, it is also heterogeneous in TME. We found the infiltrations of tumor stromal cells are different among LUAD patients, in that some patients are rich in stromal cells and others are not. We next analyzed the correlation between stromal cells and patients' clinicopathologic features. The result showed that female patients have more infiltration of many immune cell types. Previous studies have indicated that female patients have a more active immune response than male patients, which is reflected in the proliferation and activation of various immune cells, such as dendritic cells.²⁹ The differences in immune response between male and female individuals could be caused by hormone and genetic differences.³⁰ We also found that smoking increased the infiltration of plasma cells, Th2 cells, and pro-B cells, while decreasing the infiltration of conventional dendritic cells. Previous studies indicate that smoking increases the percentage of memory B cells and Th2 cells but decreases pro-B cells, and has contradictory effects in regulating dendritic cells.³¹ The effects of smoking on immune cells are complicated due to the complex compositions of cigarette, the exposure time, and quantity of smoke. The correlation between smoking and stromal cells needs further investigation in a more

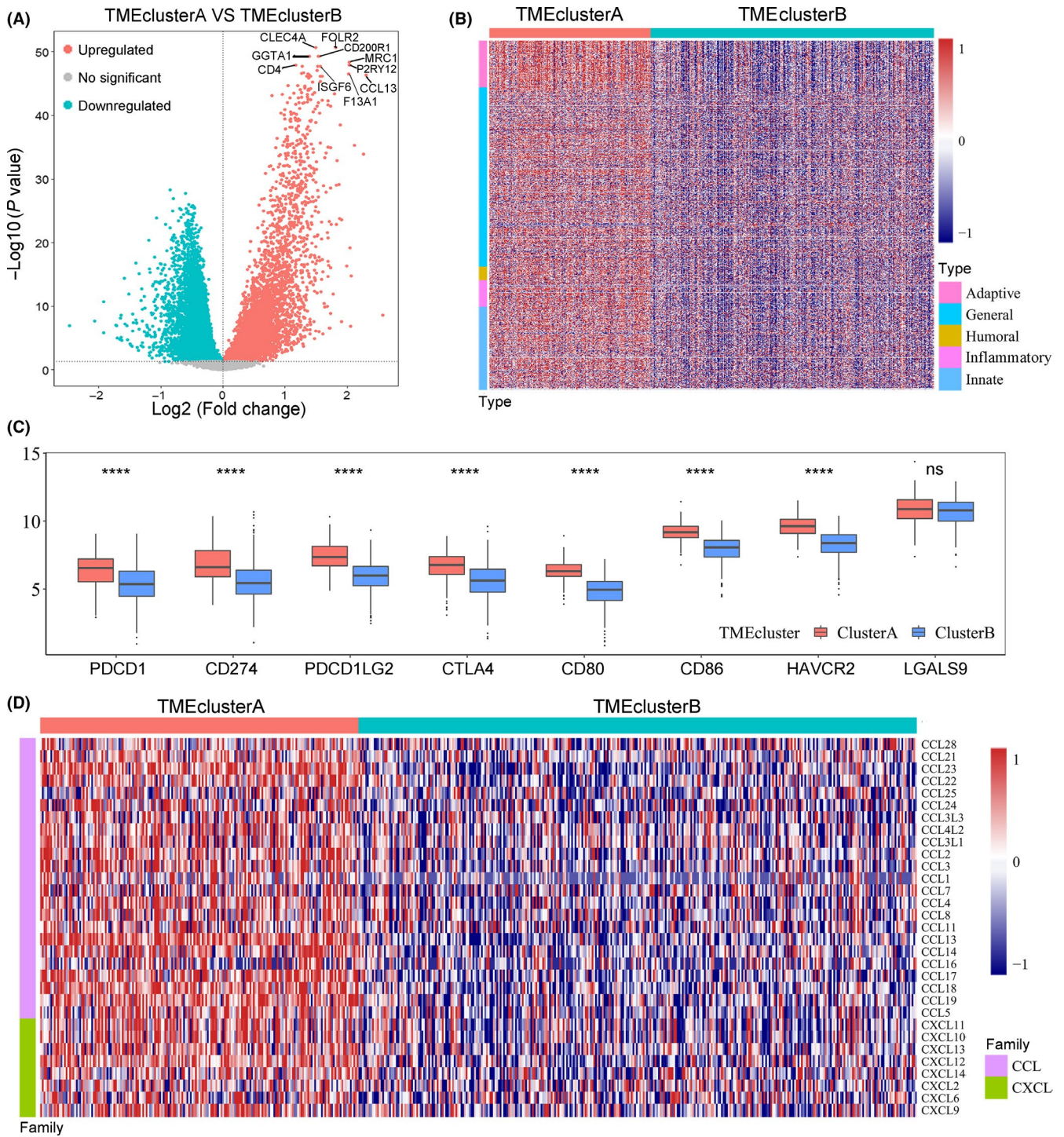


FIGURE 2 Expression pattern of immune-associated genes and chemokines in 2 tumor microenvironment (TME) subtypes. A, Differentially expressed genes in 2 TME subtypes. Differentially expressed genes, adjusted $P < .05$. Red and blue dots indicate upregulated ($N = 4409$) and downregulated ($N = 7971$) genes in TME cluster A, respectively. B, Expression pattern of 757 immune-associated genes in 2 TME subtypes. Immune-associated genes were classified into 4 immune types in the panel: innate, adaptive, humoral, and inflammatory immune response. Immune-related genes that do not belong to these 4 types are classified into the 5th class, general immune response. C, Expression pattern of immune checkpoints in 2 TME subtypes. P values obtained using Student's t test (2-tailed). **** $P < .0001$, ns, nonsignificant. D, Expression pattern of C-C motif chemokines (CCL) and C-X-C motif chemokines (CXCL) in 2 TME subtypes

specific context. Moreover, we found many immune cells decreased in advanced stage patients, including B cells, $CD4^+$ T cells, $CD8^+$ T cells, and dendritic cells, whereas some immune cells increased in advanced stage, including Th1 cells and Th2 cells. Previous studies

indicate that $CD4^+$ T cells and $CD8^+$ T cells are more abundant in early-stage cancer patients.^{32,33} Two studies suggest that B cells show no significant correlation with tumor stage in ovarian cancer and breast cancer.^{34,35} Another study suggests that B cells are correlated

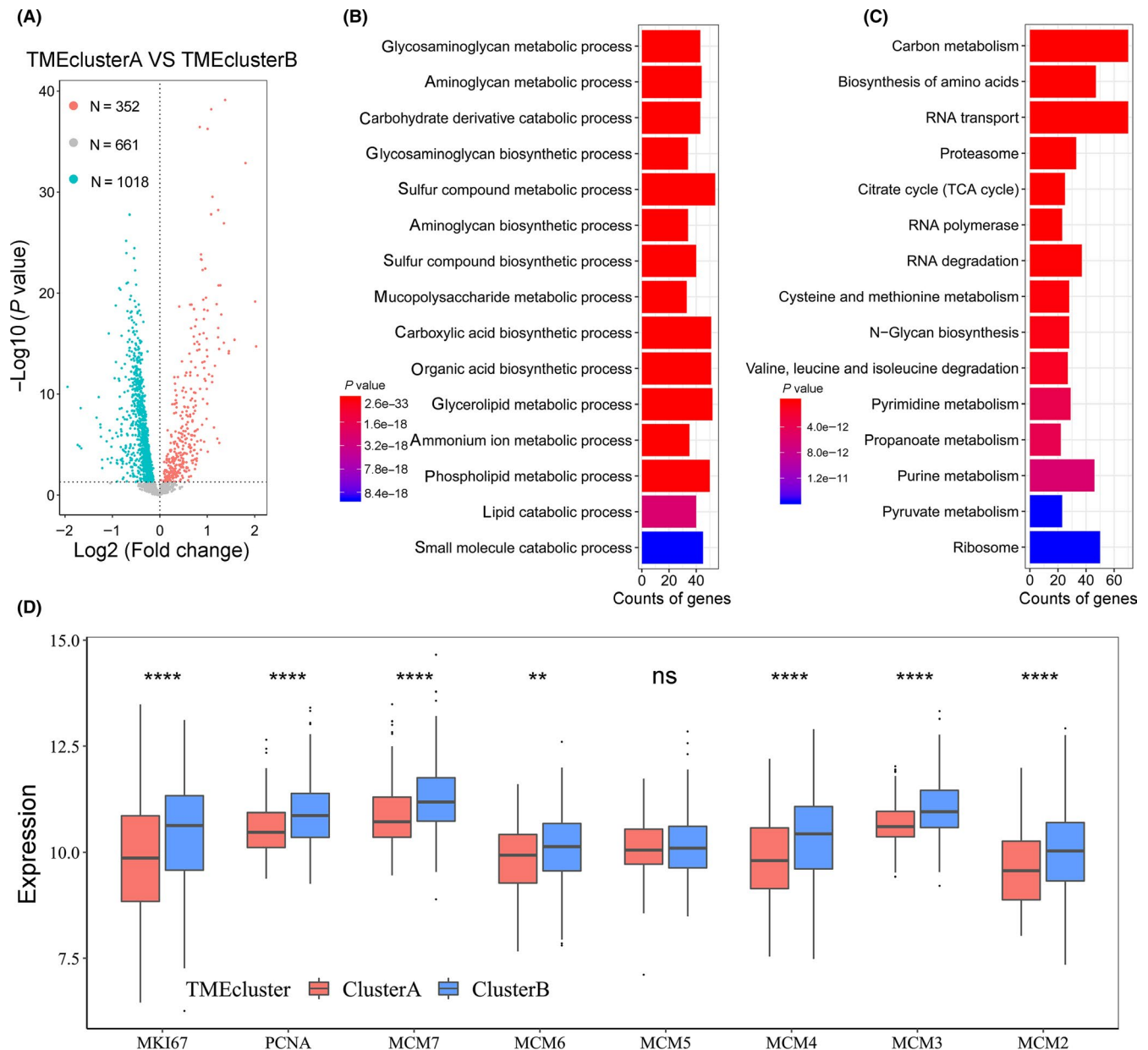


FIGURE 3 Differences in cell metabolism and proliferation markers in 2 tumor microenvironment (TME) subtypes. A, Differentially expressed metabolism genes in 2 TME subtypes. Differentially expressed genes, adjusted $P < .05$. Red and blue dots indicate upregulated (N = 352) and downregulated genes (N = 1018) in TME cluster A, respectively. B, Gene Ontology (GO) enrichment of the upregulated metabolism genes in TME subtype A. The x-axis denotes the number of genes within each GO term. C, Kyoto Encyclopedia of Genes and Genomes (KEGG) pathway enrichment of the upregulated metabolism genes in TME subtype B. The x-axis denotes the number of genes within each KEGG pathway. D, Expression pattern of proliferation markers in 2 TME subtypes. P values were obtained using Student's t test (2-tailed). ** $P < .01$, **** $P < .0001$. ns, nonsignificant

positively with lower T stage in colorectal cancer.³⁶ The correlation between B cells and tumor stage could vary in different cancers. A study reported that advanced stage patients have more abundant dendritic cells in NSCLC.³⁷ The correlation between dendritic cells and tumor stage needs further investigation. One study suggested that circulating follicular helper T cells are higher in advanced stage NSCLC.³⁸ Another 2 studies showed that circulating Th1 cells are higher in early stage NSCLC, but circulating Th2 cells are higher in advanced stage NSCLC.^{39,40} However, how tumor stage affects Th cells in the TME needs further investigation. Overall, the TME

infiltrations are largely shaped by clinicopathological characteristics of LUAD patients.

Considering the heterogeneity of stromal cells in LUAD, we used a consensus clustering algorithm to identify potential classification of LUAD based on stromal cell patterns. The clustering revealed 2 subtypes of LUAD with distinct stromal cell patterns, termed TME cluster A and TME cluster B. TME cluster A showed a more abundant infiltration of immune cells than TME cluster B. Moreover, TME cluster A showed a better clinical outcome than TME cluster B. Therefore, we hypothesized that TME cluster A

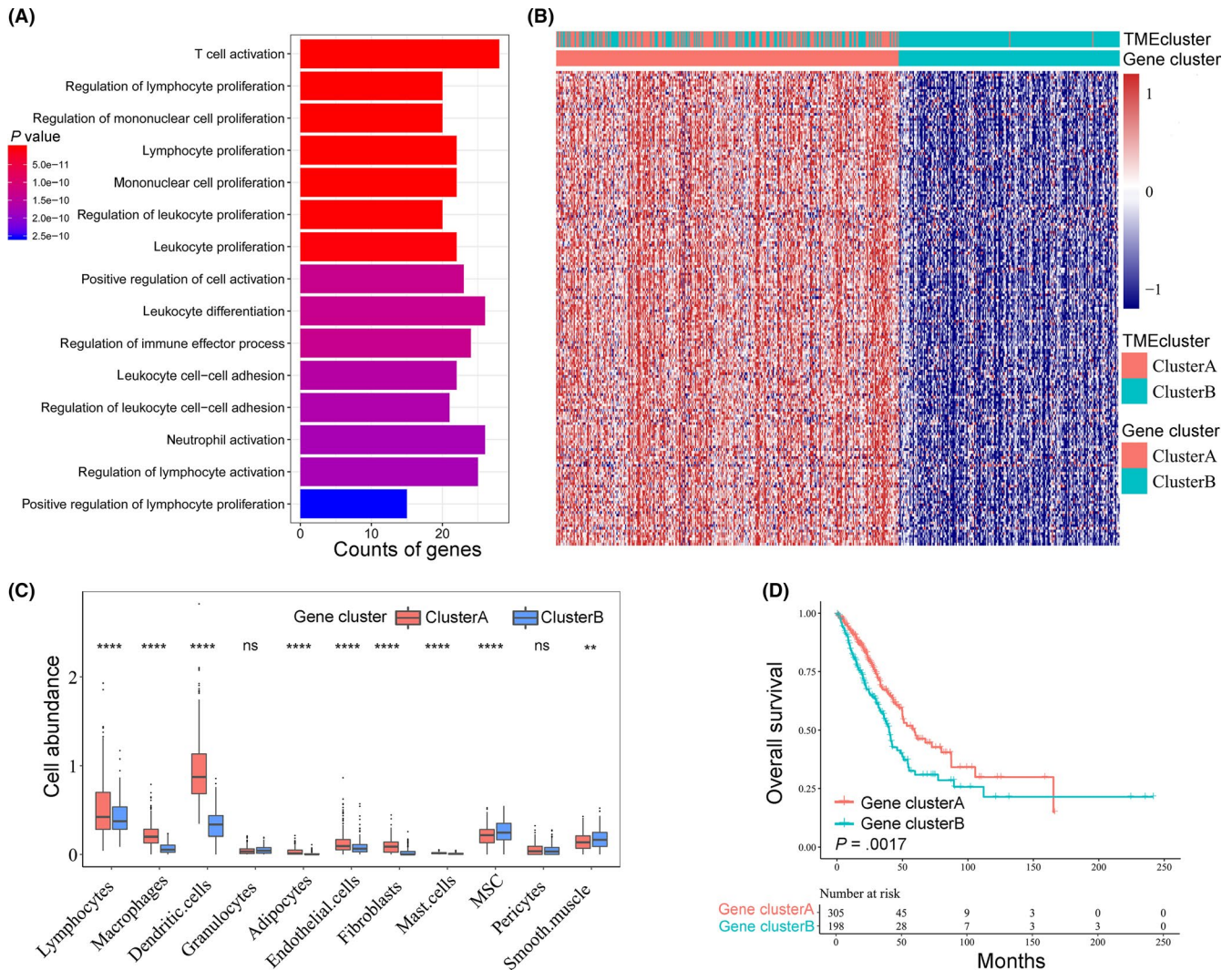


FIGURE 4 Tumor microenvironment (TME) signature genes distinguish lung adenocarcinoma patients into 2 molecular subtypes. A, Gene Ontology (GO) enrichment analysis of the upregulated TME signature genes in TME subtype A. The x-axis denotes the number of genes within each GO term. B, Unsupervised clustering of TME signature genes for 515 patients in The Cancer Genome Atlas cohort. C, TME cell abundance in different gene clusters. P values were obtained using Student's t test (2-tailed). ** $P < .01$, **** $P < .0001$. MSC, mesenchymal stem cell; ns, nonsignificant. D, Kaplan-Meier curves for overall survival of different gene subtypes. P values were obtained using the log-rank test

is an immune response active subtype and TME cluster B is an immune response repressed subtype. To further confirm the immune status of the 2 TME subtypes, we found that the overall expression of the immune-associated genes was higher in TME cluster A. These immune-associated genes were mainly expressed in immune cells, although some of them were also expressed in tumor cells. Therefore, the result suggested that immune cells in TME cluster A were more active than immune cells in TME cluster B. Furthermore, immune checkpoint genes were overexpressed in TME cluster A. Therefore, patients with TME cluster A could benefit from immune checkpoint therapy. However, this finding needs more reliable investigations, because there could be discrepancies between mRNA levels and protein levels of some immune checkpoint genes. We also found that both C-C motif chemokines and C-X-C motif chemokines were overexpressed in TME cluster A. The

C-C motif chemokines and C-X-C motif chemokines are secreted from both stromal cells and tumor cells.⁴¹ Therefore, there was a more active signal exchange through chemokines in the TME of TME cluster A. The characteristics of the cytokine/chemokine microenvironment were consistent with the stromal cell abundance in each TME subtype. Collectively, these results suggest that TME cluster A is an immune response active subtype, and TME cluster B is an immune response repressed subtype. A previous study also revealed 2 clusters of NSCLCs based on immune status; one is immune active, termed "hot" in their study, and the other is immune repressed, termed "cold".⁴²

We also analyzed the expression of metabolism-related genes in the 2 TME clusters. These metabolism-related genes mainly reflect the phenotype of tumor cells due to the sequencing data were mainly obtained from tumor cells. Therefore, tumor cells in TME

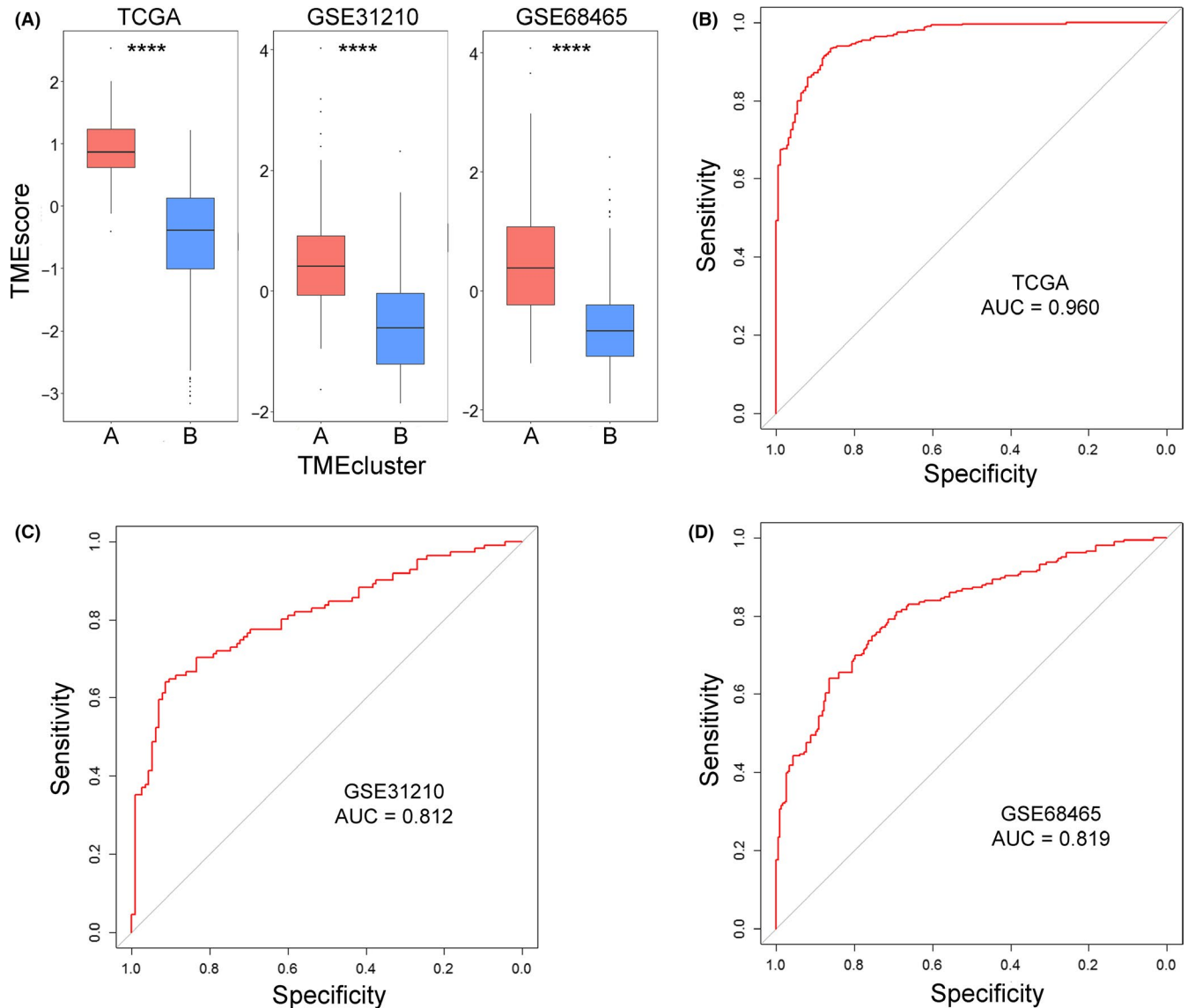


FIGURE 5 Tumor microenvironment (TME) score distinguished TME subtype in lung adenocarcinoma. A, TME score of the 2 TME clusters in 3 independent datasets: The Cancer Genome Atlas (TCGA) and 2 meta-Genes Expression Omnibus datasets (GSE31210 and GSE68465). *P* values obtained using Student's *t* test. *****P* < .0001. B, Receiver operating characteristic (ROC) measuring the diagnostic value of the TME score on TME clusters in The Cancer Genome Atlas (TCGA) dataset. Area under the ROC curve (AUC), 0.960. C, ROC measuring the diagnostic value of the TME score on TME clusters in the GSE31210 dataset. AUC, 0.812. D, ROC measuring the diagnostic value of the TME score on TME clusters in GSE68465 dataset. AUC, 0.819

cluster A were active in glycosaminoglycan, aminoglycan, and glycerolipid metabolism processes, whereas tumor cells in TME cluster B were active in diverse metabolic pathways, including carbohydrate metabolism, amino acid metabolism, nucleic acid metabolism, and the citrate cycle (TCA cycle). Tumor cells in TME cluster A showed a relatively repressed metabolic state that might be caused by the active immune response in TME cluster A. Glycosaminoglycan, aminoglycan and glycerolipid metabolism processes are associated with the ECM, which is derived from both tumor cells and stromal cells. Therefore, the result was in accordance with the more abundant stromal cells in TME cluster A. The immune repressed TME cluster B showed an enrichment in the TCA cycle. A recently published study indicates that immunosuppressive and immunodeficient

hepatocellular carcinomas show increased activity of the citrate cycle (TCA cycle) and nucleotide biosynthesis.⁴³ The TCA cycle is a classic and complicated energy metabolism cycle that involves many intermediates. The correlation among the TCA cycle, tumor cells, and immune response is complicated and is yet to be elucidated. The effects of the TCA cycle on tumor cells depends on specific metabolic intermediates and context. Succinate is one of the intermediates in the TCA cycle, which both have pro- and antitumor effects depending on the specific context.⁴⁴ Some TCA cycle intermediates are upregulated in activated leukocytes, especially in macrophages.⁴⁵ Itaconate, another intermediate in the TCA cycle, mediates cross-talk between macrophage metabolism and peritoneal tumors.⁴⁶ Therefore, the correlation between the TCA cycle

and immunosuppressive phenotype in cancer needs further investigation in a more specific context.

Moreover, our results showed that proliferation markers were underexpressed in TME cluster A than in TME cluster B. Like the metabolism-related genes, these proliferation markers mainly reflect the phenotype of tumor cells. Therefore, tumor cells in TME cluster A showed a proliferation repressed phenotype. Taken together, the immune active TME cluster A is characterized by repressed metabolism and repressed proliferation of tumor cells, whereas immune repressed TME cluster B is characterized by active metabolism and active proliferation of tumor cells. These findings also support distinct clinical outcomes of the 2 TME subtypes.

Further analysis revealed that signature genes distinguishing TME cluster A and TME cluster B were enriched in immune activation, which were significantly overexpressed in TME cluster A. Similarly, these signature genes also clustered LUAD patients into 2 clusters, termed Gene cluster A and Gene cluster B. Gene cluster A showed more abundant immune cells and a better prognosis relative to Gene cluster B. The result confirmed that signature genes distinguishing TME cluster A from TME cluster B were associated with immune activation. Finally, we constructed the TME score to diagnose the TME subtype. The TME score was significantly higher in TME cluster A than TME cluster B. The TME score showed the high diagnostic value of TME subtype in 3 independent datasets. Therefore, our data supported that the TME score distinguishes TME phenotype effectively in LUAD. Immune checkpoint genes were overexpressed in TME cluster A, which suggested TME cluster A might benefit from immune checkpoint inhibitors. We hope prospective research would correlate the expression of signature genes with the effects of immunotherapy.

In conclusion, we comprehensively analyzed the stromal cell landscape of TME in LUAD and correlated stromal cells with clinicopathologic features. Two clinically and molecularly distinct LUAD subtypes were identified based on stromal cell pattern. The 2 LUAD subtypes showed characteristic features in immune response and tumor metabolism status. Moreover, a TME signature gene score was proposed to distinguish the 2 LUAD subtypes. Based on these findings, we believe that the novel classification of LUAD might contribute to predicting clinical outcome and guide immunotherapy. Further prospective studies are warranted to validate the clinical value of this classification.

ACKNOWLEDGMENTS

This work was supported by the National Natural Science Foundation of China (81802299 and 81502514), the CAMS Innovation Fund for Medical Sciences (2016-I2M-1-001 and 2017-I2M-1-005), the Fundamental Research Funds for the Central Universities (3332018070), the National Key Research and Development Program of China (2016YFC0901401), and the National Key Basic Research Development Plan (2018YFC1312105). Jianbing Huang also wishes to thank the support and care from Huiyu Feng.

CONFLICT OF INTEREST

The authors declare that no conflict of interest exists.

ORCID

Shuangshuang Mao  <https://orcid.org/0000-0001-6799-5813>

Jie He  <https://orcid.org/0000-0002-0285-5403>

REFERENCES

- Remark R, Becker C, Gomez JE, et al. The non-small cell lung cancer immune contexture. A major determinant of tumor characteristics and patient outcome. *Am J Respir Crit Care Med.* 2015;191:377-390.
- Quail DF, Joyce JA. Microenvironmental regulation of tumor progression and metastasis. *Nat Med.* 2013;19:1423-1437.
- Fridman WH, Pages F, Sautes-Fridman C, Galon J. The immune contexture in human tumours: impact on clinical outcome. *Nat Rev Cancer.* 2012;12:298-306.
- Fridman WH, Zitvogel L, Sautes-Fridman C, Kroemer G. The immune contexture in cancer prognosis and treatment. *Nat Rev Clin Oncol.* 2017;14:717-734.
- Rosenberg JE, Hoffman-Censits J, Powles T, et al. Atezolizumab in patients with locally advanced and metastatic urothelial carcinoma who have progressed following treatment with platinum-based chemotherapy: a single-arm, multicentre, phase 2 trial. *Lancet.* 2016;387:1909-1920.
- Jiang Y, Zhang Q, Hu Y, et al. ImmunoScore signature: a prognostic and predictive tool in gastric cancer. *Ann Surg.* 2018;267:504-513.
- Lievense LA, Sterman DH, Cornelissen R, Aerts JG. Checkpoint blockade in lung cancer and mesothelioma. *Am J Respir Crit Care Med.* 2017;196:274-282.
- Tang H, Qiao J, Fu YX. Immunotherapy and tumor microenvironment. *Cancer Lett.* 2016;370:85-90.
- Klemm F, Joyce JA. Microenvironmental regulation of therapeutic response in cancer. *Trends Cell Biol.* 2015;25:198-213.
- Altorki NK, Markowitz GJ, Gao D, et al. The lung microenvironment: an important regulator of tumour growth and metastasis. *Nat Rev Cancer.* 2019;19:9-31.
- Mariathasan S, Turley SJ, Nickles D, et al. TGFbeta attenuates tumour response to PD-L1 blockade by contributing to exclusion of T cells. *Nature.* 2018;554:544-548.
- Li Y, Lu Z, Che Y, et al. Immune signature profiling identified predictive and prognostic factors for esophageal squamous cell carcinoma. *Oncoimmunology.* 2017;6:e1356147.
- Bray F, Ferlay J, Soerjomataram I, Siegel RL, Torre LA, Jemal A. Global cancer statistics 2018: GLOBOCAN estimates of incidence and mortality worldwide for 36 cancers in 185 countries. *CA: Cancer J Clin.* 2018;68:394-424.
- Chen Z, Fillmore CM, Hammerman PS, Kim CF, Wong KK. Non-small-cell lung cancers: a heterogeneous set of diseases. *Nat Rev Cancer.* 2014;14:535-546.
- Aran D, Hu Z, Butte AJ. xCell: digitally portraying the tissue cellular heterogeneity landscape. *Genome Biol.* 2017;18:220.
- Gautier L, Cope L, Bolstad BM, Irizarry RA. affy-analysis of Affymetrix GeneChip data at the probe level. *Bioinformatics.* 2004;20:307-315.
- Wilkerson MD, Hayes DN. ConsensusClusterPlus: a class discovery tool with confidence assessments and item tracking. *Bioinformatics.* 2010;26:1572-1573.
- Ritchie ME, Phipson B, Wu D, et al. limma powers differential expression analyses for RNA-sequencing and microarray studies. *Nucleic Acids Res.* 2015;43:e47.
- Kursa MB, Rudnicki WR. Feature Selection with the Boruta package. *J Stat Softw.* 2010;36.

20. Yu G, Wang LG, Han Y, He QY. clusterProfiler: an R package for comparing biological themes among gene clusters. *OmicS*. 2012;16:284-287.
21. Sotiriou C, Wirapati P, Loi S, et al. Gene expression profiling in breast cancer: understanding the molecular basis of histologic grade to improve prognosis. *J Natl Cancer Inst*. 2006;98:262-272.
22. Zeng D, Li M, Zhou R, et al. Tumor microenvironment characterization in gastric cancer identifies prognostic and immunotherapeutically relevant gene signatures. *Cancer Immunol Res*. 2019;7:737-750.
23. Robin X, Turck N, Hainard A, et al. pROC: an open-source package for R and S+ to analyze and compare ROC curves. *BMC Bioinformatics*. 2011;12.
24. Cesano A. nCounter(R) pancancer immune profiling panel (NanoString Technologies Inc, Seattle, WA). *J Immunother Cancer*. 2015;3:42.
25. O'Neill LA, Kishton RJ, Rathmell J. A guide to immunometabolism for immunologists. *Nat Rev Immunol*. 2016;16:553-565.
26. Kim P, Cheng F, Zhao J, Zhao Z. ccmGDB: a database for cancer cell metabolism genes. *Nucleic Acids Res*. 2016;44:D959-D968.
27. Jurikova M, Danihel L, Polak S, Varga I. Ki67, PCNA, and MCM proteins: Markers of proliferation in the diagnosis of breast cancer. *Acta Histochem*. 2016;118:544-552.
28. Batista PJ, Chang HY. Long noncoding RNAs: cellular address codes in development and disease. *Cell*. 2013;152:1298-1307.
29. Bengtsson AK, Ryan EJ, Giordano D, Magaletti DM, Clark EA. 17beta-estradiol (E2) modulates cytokine and chemokine expression in human monocyte-derived dendritic cells. *Blood*. 2004;104:1404-1410.
30. Oertelt-Prigione S. The influence of sex and gender on the immune response. *Autoimmun Rev*. 2012;11:A479-A485.
31. Qiu F, Liang CL, Liu H, et al. Impacts of cigarette smoking on immune responsiveness: Up and down or upside down? *Oncotarget*. 2017;8:268-284.
32. Zhou L, Li Y, Gao W, et al. Assessment of tumor-associated immune cells in laryngeal squamous cell carcinoma. *J Cancer Res Clin Oncol*. 2019;145:1761-1772.
33. Goepfert B, Frauenschuh L, Zucknick M, et al. Prognostic impact of tumour-infiltrating immune cells on biliary tract cancer. *Br J Cancer*. 2013;109:2665-2674.
34. Lundgren S, Berntsson J, Nodin B, Micke P, Jirstrom K. Prognostic impact of tumour-associated B cells and plasma cells in epithelial ovarian cancer. *J Ovarian Res*. 2016;9:21.
35. Mehdipour F, Razmkhah M, Faghih Z, Bagheri M, Talei AR, Ghaderi A. The significance of cytokine-producing B cells in breast tumor-draining lymph nodes. *Cell Oncol*. 2019;42:381-395.
36. Berntsson J, Nodin B, Eberhard J, Micke P, Jirstrom K. Prognostic impact of tumour-infiltrating B cells and plasma cells in colorectal cancer. *Int J Cancer*. 2016;139:1129-1139.
37. Minkov P, Gulubova M, Ivanova K, Obretenov E, Ananiev J. CD11c- and CD123-positive dendritic cells in development of antitumour immunity in non-small cell lung cancer patients. *Polish J Pathol*. 2019;70:109-114.
38. Guo Z, Liang H, Xu Y, et al. The role of circulating T follicular helper cells and regulatory cells in non-small cell lung cancer patients. *Scand J Immunol*. 2017;86:107-112.
39. Qiu L, Yu Q, Zhou Y, et al. Functionally impaired follicular helper T cells induce regulatory B cells and CD14(+) human leukocyte antigen-DR(-) cell differentiation in non-small cell lung cancer. *Cancer Sci*. 2018;109:3751-3761.
40. Hu X, Gu Y, Zhao S, Hua S, Jiang Y. Elevated circulating CD4(+) CD25(-)Foxp3(+) regulatory T cells in patients with nonsmall cell lung cancer. *Cancer Biother Radiopharm*. 2019;34:325-333.
41. Vinader V, Afarinkia K. The emerging role of CXC chemokines and their receptors in cancer. *Fut Med Chem*. 2012;4:853-867.
42. Lizotte PH, Ivanova EV, Awad MM, et al. Multiparametric profiling of non-small-cell lung cancers reveals distinct immunophenotypes. *JCI Insight*. 2016;1:e89014.
43. Zhang Q, Lou Y, Yang J, et al. Integrated multiomic analysis reveals comprehensive tumour heterogeneity and novel immunophenotypic classification in hepatocellular carcinomas. *Gut*. 2019;1-13.
44. Jiang S, Yan W. Succinate in the cancer-immune cycle. *Cancer Lett*. 2017;390:45-47.
45. Patil NK, Bohannon JK, Hernandez A, Patil TK, Sherwood ER. Regulation of leukocyte function by citric acid cycle intermediates. *J Leukoc Biol*. 2019;106:105-117.
46. Weiss JM, Davies LC, Karwan M, et al. Itaconic acid mediates cross-talk between macrophage metabolism and peritoneal tumors. *J Clin Invest*. 2018;128:3794-3805.

SUPPORTING INFORMATION

Additional supporting information may be found online in the Supporting Information section.

How to cite this article: Huang J, Li J, Zheng S, et al. Tumor microenvironment characterization identifies two lung adenocarcinoma subtypes with specific immune and metabolic state. *Cancer Sci*. 2020;111:1876-1886. <https://doi.org/10.1111/cas.14390>